# AND TRAINING

# MINISTRY OF EDUCATION VIETNAM ACADEMY OF SCIENCE AND TECHNOLOGY

# GRADUATE UNIVERSITY OF SCIENCE AND ECHNOLOGY



# Ngo Nhu Viet

# INVESTIGATING ELECTROMAGNETIC WAVE ABSORPTION PROPERTIES VIA RESONANT INTERACTION IN MULTILAYER METAMATERIALS

SUMMARY OF DISSERTATION ON MATERIALS SCIENCE

Major: Electronic material

Code: 9 44 01 23

Ha Noi - 2025

The dissertation is completed at: Graduate University of Science and
Technology, Vietnam Academy Science and Technology

# Supervisors:

- 1. Supervisor 1: Dr. Bui Son Tung, Graduate University of Science and Technology, Vietnam Academy Science and Technology
- 2. Supervisor 2: Prof. Dr. Vu Dinh Lam, Graduate University of Science and Technology, Vietnam Academy Science and Technology

Referee 1:	 	
Referee 2:	 	

The dissertation is examined by Examination Board of Graduate University of Science and Technology, Vietnam Academy of Science and Technology at...... (time, date.....)

The dissertation can be found at:

- 1. Graduate University of Science and Technology Library
- 2. National Library of Vietnam

#### INTRODUCTION

# 1. The urgency of the dissertation

Metamaterial absorbers (MA) are engineered materials designed to efficiently absorb electromagnetic waves in specific frequency ranges [10–12]. Their micro-structured designs enable control of wave absorption beyond natural materials. First introduced by Landy, research on MAs has rapidly expanded, with applications in both THz and GHz bands. A typical MA consists of a resonant layer, a dielectric spacer, and a metallic ground plane.

Single-layer MA usually provide strong absorption at one frequency but have limited tunability and are sensitive to incident angle and polarization. To address these limitations, multilayer metamaterial absorbers (MMA) were developed. By adjusting layer thickness, stacking, and design, MMA can achieve broader or narrower absorption bands, improve efficiency, and enhance stability against angle and polarization variations [18–19].

Research into MMA can achieve desirable properties such as broadband and multi-peak absorption, thereby offering numerous applications for this material in areas like energy harvesting, electromagnetic shielding, and sensing... Thus, the project entitled: "Investigating Electromagnetic Wave Absorption Properties via Resonant Interaction in Multilayer Metamaterials" was chosen. This dissertation topic introduces novel and unique contributions within the Vietnamese research landscape on MA, distinguishing itself from prior studies [17], [22-25]. While these previous studies covered a range of MA subjects, they predominantly addressed single-layer MA structures. This thesis, however, specifically focuses on MMA to elucidate their absorption mechanisms and characteristics.

# 2. The objectives of the dissertation

- Design and Analysis: To design MMA capable of multi-band and broadband absorption, and to explore the possibility of switching between EIT (Electromagnetically Induced Transparency) and EIA (Electromagnetically Induced Absorption).
- Mechanism Elucidation: To clarify the mechanism of interaction between the layers within the structure.
- Role of Losses: To elucidate the role of material loss components (Ohmic and dielectric losses) in the overall performance.

#### 3. Content of the Research

The thesis involved designing and simulating MMA structures using CST software, and fabricating them through photolithography. A combined methodology of calculation, simulation, and experimental measurement was employed to evaluate the electromagnetic properties (absorption, reflection, and transmission). The scope of the research focuses on the interaction between layers within the MMA in the GHz and THz frequency ranges.

# 4. Scientific and Practical Implications

This research has scientific merit by modeling and elucidating the operational mechanisms and interlayer interactions within MMA structures. Practically, the findings offer valuable contributions toward the application of MMA in fields such as energy harvesting, electromagnetic shielding, and sensing.

#### **Novel Contributions**

In this thesis, several MMA structures were successfully proposed and fabricated. These MMA structures were designed based on the principle of electromagnetic resonance at specific frequencies, where the dielectric and conductive layers play a key role in tuning the absorption bandwidth.

The interaction mechanism between the structural layers was elucidated through investigations of the absorption spectrum, surface current distribution, magnetic field, and electric field in the MMA samples. Simulation results indicate the potential for expanding MMA applications, particularly in broadband absorption, polarization tuning, and optoelectronic sensor integration.

Furthermore, the dissertation also involved the study and simulation of multifunctional MMA structures, demonstrating the ability to switch between EIT and EIA effects.

#### **Thesis Structure**

The dissertation comprises 140 pages, including an Introduction, five content chapters, and the Conclusions.

# CHAPTER 1. OVERVIEW OF MULTILAYER METAMATERIAL ABSORBERS OF ELECTROMAGNETIC WAVES

# 1.1. Introduction to electromagnetic wave metamaterial absorbers

# 1.1.1. Metamaterials: a general overview

Metamaterials (MM), named from the Greek for "beyond" are synthetic composites made from materials like plastics and metals. Their electromagnetic properties arise from the geometry of engineered subwavelength structures rather than their chemical makeup. By designing periodic patterns, key parameters such as permittivity, permeability, and refractive index can be precisely controlled. Due to their remarkable characteristics, MMs are now employed across numerous applications, including superlenses [7], [29], [30], invisibility cloaks [8], [31], [32], perfect absorbers (MPA) [9], [33], [34], and sensors [35], [36], [37]...

## 1.1.2. Definition, classification, and evolution of metamaterial absorbers

MA is an MM variant specially engineered for effective electromagnetic energy absorption across specific frequency ranges. Its absorption performance is predominantly dictated by its artificial microstructure, rather than its constituent chemical elements.

MA can be classified according to various criteria. Specifically, they can be divided into broad-band and narrow-band, depending on their absorption bandwidth [38], [39]. Additionally, Metamaterial Absorbers can be categorized based on their operating frequency range, including MA working in the microwave, THz, and optical regions.

# 1.2. Mechanism of operation for metamaterial absorbers

# 1.2.1. Electric and magnetic resonances in metamaterials

Magnetic resonance results from the array's geometric interaction with the incident wave's magnetic component. At resonance, this interaction induces displacement or circulating currents within the structure, creating a strong effective magnetic response, which can cause the effective permeability (μ) to become negative [44], [45].

Magnetic resonance occurs through the generation of induced circulating currents in loop-like elements, such as SRRs or closed/semi-closed loops, upon interaction with the incident wave's magnetic field component. At resonance, these eddy currents are highly amplified, creating a secondary induced magnetic field. This field can lead to the phenomenon of negative magnetic permeability ( $\mu$ ), a unique property not found in natural materials [45], [46].

## 1.2.2. Impedance matching theory

Impedance matching aims to tune the electromagnetic characteristics of the MA so that its impedance closely matches the wave impedance of the surrounding medium. This minimizes reflection at the surface and

maximizes the transmission of energy into the absorbing layer. Once the electromagnetic wave enters the material, its energy is further dissipated through internal loss processes, which are determined by the geometric design and electromagnetic parameters of each structural component.

# 1.2.3. Energy dissipation mechanisms in metamaterials

Dielectric loss occurs in the non-conductive host material, where energy is dissipated when polarizing dipoles oscillate or reorient in response to the applied external electric field. As the electromagnetic wave interacts with the material, these dipoles undergo vibration and lose energy via internal molecular friction, which manifests as heat [53].

Ohmic loss primarily occurs in the thin metallic layers of the MA. When an electromagnetic wave reaches the conductive layer, it activates induced currents-currents that are forced to oscillate by the incident wave field. This process generates heat due to the metal's internal resistance within the MA structure.

# 1.3. Multilayer metamaterial absorbers of electromagnetic waves

## 1.3.1. Broadband multilayer metamaterial absorbers

The stacking of layers in MMA plays a crucial role in broadening the absorption bandwidth and enhancing the material's efficiency. Each layer in the multilayer structure typically includes distinct resonant elements, such as small metallic patterns or graphene structures placed on a dielectric substrate. When these layers are stacked, they create multi-level resonances with various resonance points, corresponding to multi-band or broadband absorption frequencies [58], [77-78].

# 1.3.2. Multifunctional multilayer metamaterials

Furthermore, MMA are employed to obtain enhanced absorption at multiple distinct frequencies [61]. The increased absorption capability in MMA can be achieved by switching between EIT and EIA effects [61], [84]

# 1.3.3. Applications of multilayer electromagnetic wave absorbing metamaterials

MA can be engineered using multilayer configurations comprising diverse materials to optimize the absorbing structure and enhance their absorption capabilities [88], [89], or to provide effective shielding against electromagnetic radiation [90]. These MMA find applications across various fields, including energy harvesting [91] and sensing [92].

# 1.4. Conclusion of Chapter 1

This chapter presents the fundamentals of MAs. It then analyzes and evaluates their operating mechanisms, including electric and magnetic resonance, impedance matching, and energy dissipation theory. Additionally, the chapter introduces various MMA structures with different mechanisms and discusses several key MMA applications.

#### CHAPTER 2. RESEARCH METHODOLOGY

#### 2.1. Theoretical research method

# 2.1.1. Simulation methodology

Specialized software packages such as CST Microwave Studio, HFSS, and COMSOL are commonly used to design and simulate MM. They allow for the simulation of materials in either 2D or 3D space. The electromagnetic properties of an MM can be determined by simulating a single unit cell structure, completely defining the parameters, material types, and appropriate boundary conditions.

# 2.1.2. Equivalent LC circuit model

The electromagnetic properties of MA can be predicted and explained based on the equivalent RLC circuit model. The RLC circuit model depends on the MA's structural configuration, where the metallic layers are replaced by inductors with effective inductance L and capacitors with effective capacitance C. The values of L and C are calculated based on the structural geometry and the electromagnetic energy distribution. Each metal-dielectric layer corresponds to a single RLC circuit, and consequently, an MMA structure is modeled as a series of RLC circuits [87], [93-95].

## 2.1.3. Coupled oscillator model

EIT is understood as a quantum interference phenomenon between different excitation sources. Initially, a first excitation source is introduced into the medium, which absorbs waves from this source as the medium is considered opaque to it. Subsequently, the medium is simultaneously subjected to a second excitation source, from which it can also absorb waves. At this point, an interference effect occurs that converts the absorption property into a transmission property, and vice versa [97-99].

#### 2.2. Fabrication method

Photolithography is a pervasive material fabrication technique enabling the creation of precisely shaped and sized features. Its principle relies on using light radiation to change the characteristics of a photoresist layer coated on the material surface. The photoresist, a photosensitive organic compound, remains robust in alkaline or acidic media, protecting the material details from subsequent etching.

# 2.3. Measurement method for electromagnetic properties of multilayer metamaterials

The Vector Network Analyzer (VNA) system at the Institute of Materials Science, Vietnam Academy of Science and Technology, is used to

determine the reflectance and transmittance of MA and MMA. This system features two antennas serving as the source and receiver, whose positions are adjusted based on the required measurement. The output of the measurement is the complex S-parameters, which characterize the reflective and transmissive properties of the MA and MMA.

## 2.4. Conclusion of Chapter 2

The CST Microwave Studio software is used to optimally design the MA and MMA structures. Computational methods are implemented to compare, correlate, and further optimize these designs. Based on both simulation and calculation, the MMA are fabricated primarily via photolithography and other methods. Post-fabrication, the electromagnetic properties of the samples are measured using a Vector Network Analyzer (VNA) system. The resulting experimental data is then compared and correlated with the simulation and computational findings.

# CHAPTER 3. INTERLAYER INTERACTION EFFECTS ON ABSORPTION PROPERTIES OF MULTILAYER METAMATERIALS IN THE GHZ RANGE

#### 3.1. Effect of metal on interaction

#### 3.1.1. MMA with low ohmic loss

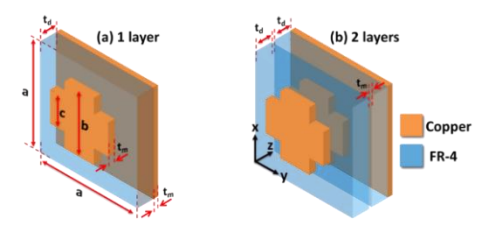


Figure 3.1. Simulated Structure: (a) Single-Layer and (b) MMA

A MA comprises a metal-dielectric layer situated on a continuous metallic backplate, with a unit cell size of a. The MMA is created by

increasing the number of these metal-dielectric layers. In the metal-dielectric layer, the metal component is patterned with a cross-shaped structure having a thickness of  $t_m$ , a length of b, and a width of c, and it is placed on a continuous dielectric substrate of thickness  $t_d$ . The continuous metallic backplate at the bottom has a thickness of  $t_b$ . The structural parameters of the unit cell are set as follows: a = 18 mm, b = 16 mm, c = 7 mm,  $t_b = 0.035$  mm, and  $t_m = 0.035$  mm. The dielectric material used is FR-4, with a relative permittivity of  $\varepsilon = 4.3$  and a loss tangent of  $\tan \delta = 0.025$ . The metallic layers are made of copper with an electrical conductivity of  $\sigma = 5.96$  ×  $10^7$  S/m.

The MMA structure yields an absorption spectrum with absorption exceeding 90% in the frequency range of 4.84–5.02 GHz, as shown in Figure 3.2(a). There are two maximum absorption peaks at 4.89 GHz and 4.97 GHz, with absorption values of 98.99% and 98.44%, respectively.

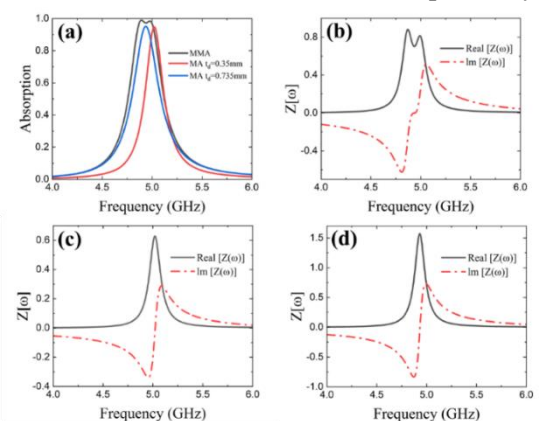


Figure 3.2. (a) Absorption spectra of the multilayer MA and single-layer ones with two different die- lectric layer thicknesses. (b) Effective impedance of the multilayer MA, and single-layer ones with td = (c) 0.35 and (d) 0.735 mm.

The equivalent circuit model for the MMA is illustrated in Figure 3.10(a). Figure 3.10(b) presents the calculated spectrum of the total current

for the circuit model for both the single-layer MA and the MMA. In the case of the MA, a single absorption peak appears at 4.95 GHz. Conversely, for the MMA, the shape of the calculated spectrum aligns with the shape of the simulated absorption spectrum, showing two distinct peaks at 4.73 GHz and 5.01 GHz. A comparison of the experimental and simulated absorption spectra for the MA and MMA is provided in Figures 3.10(c) and 3.10(d). For the MA structure, both simulation and experimental results show a single peak at 5.02 GHz and 5 GHz, with absorption values of 94.7% and 90.3%, respectively. For the MMA, in the simulation, the proposed multilayer structure achieves an absorption greater than 90% in the frequency range of 4.84–5.02 GHz. The experimental absorption reaches 90% over a broader frequency range of 4.72–5.18 GHz.

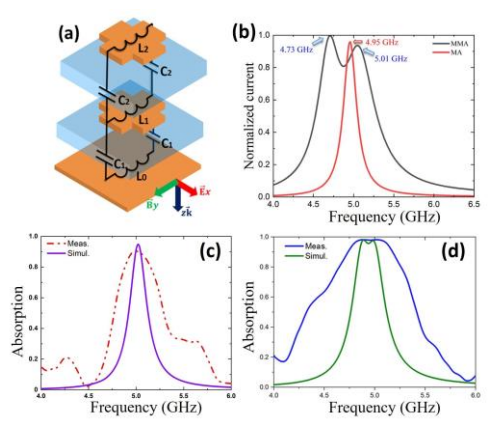
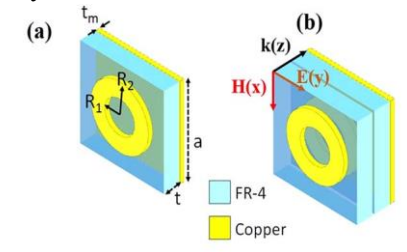


Figure 3.10. (a) Equivalent-circuit models of the MMA. (b) Calculation of the normalized total current in the single MA and MMA, according to the LC circuit model. Measured and simulated absorption spectra of (c) the single-layer and (d) MMA

The MMA proposed consists of two circular ring-shaped resonant layers (Figure 3.11). Under normal incidence, the proposed MMA exhibits an absorption peak at 4.31 GHz with an absorption rate of 98.9%. The proposed multilayer MMA is characterized by its insensitivity to the angle

of incidence for both mode TE and TM polarizations. The unit cell size is a = 20 mm. The metallic resonant structure is designed as a circular resonant ring with a thickness of  $t_m = 0.036$  mm, an outer radius of  $R_1 = 8.5$  mm, and an inner radius of  $R_2 = 2.5$  mm. The dielectric material used is FR-4, which has a relative permittivity of  $\varepsilon = 4.3$  and a loss tangent of  $\tan \delta = 0.025$  with a thickness of t = 0.9 mm. The metallic layers are made of copper, with an electrical conductivity of  $\sigma = 5.96 \times 10^7$  S/m.



**Figure 3.16.** (a) Simulated and (b) experimental absorption spectra of the MMA at various incidence angles under TE polarization, including 10°, 30°, 50°, and 70°

At normal incidence, the absorption rate increases from 93.1% (single-layer) to 98.9% (multilayer), and the MMA maintains its absorption peak intensity at approximately 97.5% even when the incidence angle is 70°. Under obliquely incident TM polarized waves, the absorption peak is still observed, but the absorption gradually decreases.

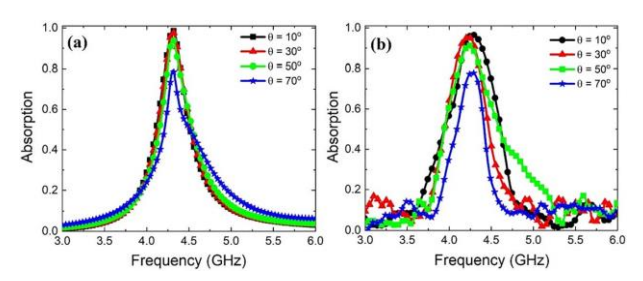


Figure 3.17. (a) Simulated and (b) experimental absorption spectra of the MMA at various incidence angles under TM polarization, including 10°, 30°, 50° và 70°.

# 3.1.2. MMA exhibits high ohmic losses

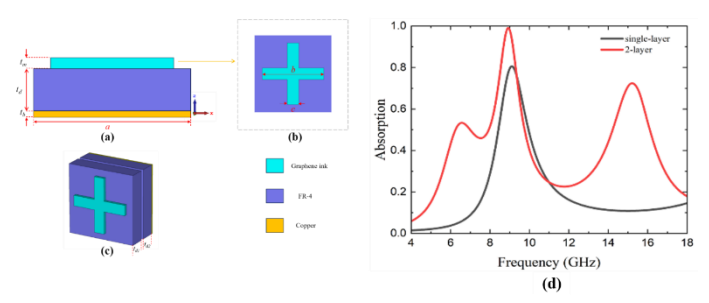


Figure 3.18. Proposed MA and MMA structures: (a) Single-layer MA, (b) Resonant layer design, (c) MMA, and (d) Absorption spectrum of MA and MMA with a Graphene absorber layer  $(2\Omega/sq)$ .

The MA structure comprises a cross-shaped graphene layer with length b, width c, and thickness  $t_g$  (Figure 3.18 b), and an FR-4 dielectric layer with thickness  $t_d$  placed atop a continuous copper metallic plate of thickness  $t_m$ . The unit cell size is a. FR-4 is used with a dielectric constant  $\varepsilon$  = 4.3 and a loss tangent of 0.025. The electrical conductivity of copper is  $5.96 \times 10^7$  S/m, while the conductive graphene ink has a varying surface resistance. Figure 3.18 c depicts the MMA structure, which consists of two graphene-FR-4 layers of the same dimensions and design as the MA, placed on a continuous copper metallic plate.

Figure 3.18 d shows that the graphene MA exhibits one absorption peak at a frequency of 9.1 GHz with a relatively low absorbance of 80.55%. When the number of layers increases to two, the number of absorption peaks rises to three within the 4–18 GHz frequency range.

The MA structure exhibits an absorption spectrum with a peak at a frequency of 9.57 GHz, reaching an absorbance of 99.57%. Concurrently, the structure also achieves an absorption bandwidth of 5.22 GHz, with the absorbance exceeding 90% within the 7.37–12.59 GHz frequency range. The MMA structure features absorption peaks at 8GHz and 12.16 GHz, reaching 96.86% and 98.29%, respectively. This structure demonstrates a broad absorption bandwidth exceeding 8.43GHz, with the absorbance surpassing 90% in the 6.07–14.5GHz frequency band.

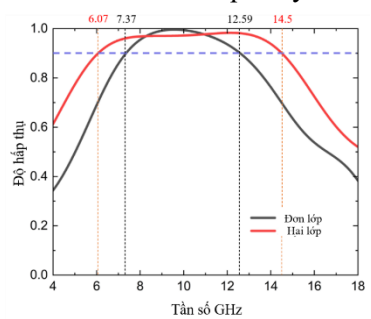


Figure 3.24. Absorption spectra of MA ( $t_d$ =3.5mm) and MMA ( $t_{d1}$ = $t_{d2}$ =1.7mm) with a graphene absorber layer ( $100\Omega$ /sq.)

Figure 3.36a illustrates the experimental and simulated absorption spectra of the proposed MMA structure. The simulated and experimental results show excellent agreement, confirming that the fabricated MMA structure achieves an absorbance exceeding 90% in the 5.43 to 13.65GHz frequency range.

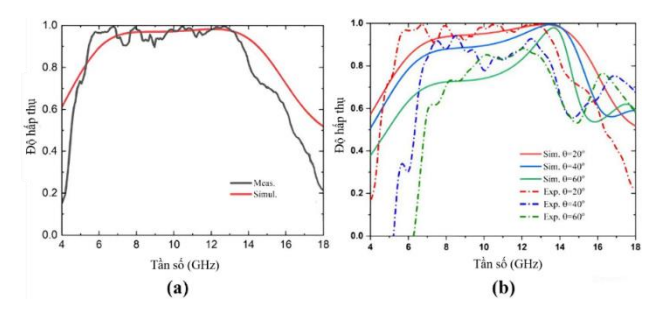


Figure 3.36. (a) Experimental and simulated absorption spectra of graphene MMA. (b) Experimental absorption spectra of graphene MMA at various incidence angles.

#### 3.2. Influence of the dielectric on the interaction

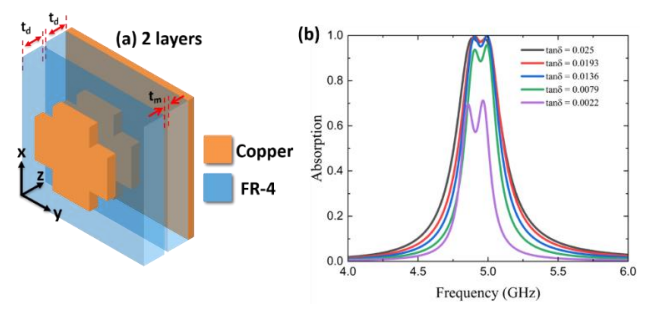


Figure 3.37. (a) Schematic of the MMA structure, (b) Absorption spectra of MMA with varying tanô (loss tangent).

As shown in Figure 3.37, observing the absorption spectra of the MMA structure reveals that the absorbance gradually decreases as the dielectric loss tangent ( $\tan\delta$ ) is reduced from 0.025 to 0.0022. At frequencies of 4.85 GHz and 4.96 GHz, the absorbance reaches 69.67% and 71.26% when  $\tan\delta$ =0.0022. The results clearly indicate the influence of the dielectric, or more specifically, the dielectric loss, on the absorption capability of the MMA structure.

The structural parameters of the unit cell are set as a=18mm, b=16mm, c=7mm,  $t_b=0.035$ mm,  $t_d=0.035$ mm, and  $t_m=0.035$ mm. The absorption spectra of the MA and MMA structures are presented in Figure

3.38 c. The MA exhibits an absorption peak at a frequency of 3.13GHz with an absorbance of 89.94%. The absorption spectrum of the MMA structure shows two absorption peaks, reaching 95.1% and 69.41% at frequencies of 3.03 GHz and 3.14 GHz, respectively.

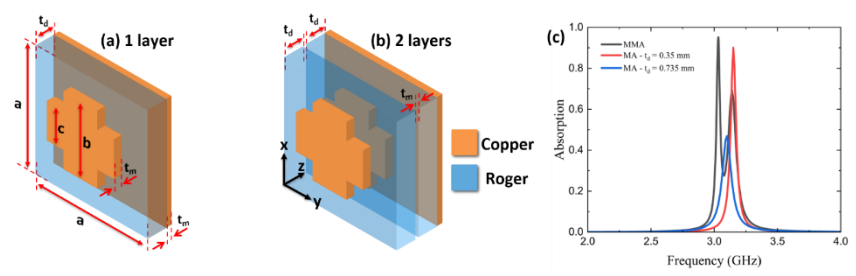


Figure 3.38. (a) Schematic of the Single-layer MA structure, (b) MMA structure, and (c) Absorption spectra of MA and MMA.

# 3.3. Conclusion of Chapter 3

The chapter successfully designed, simulated, and fabricated a two-layer, cross-shaped copper MMA, achieving 90% absorbance within the 4.84–5.02GHz range. A copper metal ring MMA structure was also presented, showing a 98.9% peak absorbance at 4.31GHz and maintaining high performance at large incidence angles. The study further proposed an MMA with low dielectric and ohmic losses to clearly clarify the influence of these losses on the overall absorption capability.

CHAPTER 4. THE INFLUENCE OF INTER-LAYER INTERACTION ON THE ABSORPTION PROPERTIES OF MULTILAYER METAMATERIALS IN THE THZ FREQUENCY RANGE

#### 4.1. Influence of the metal on the interaction

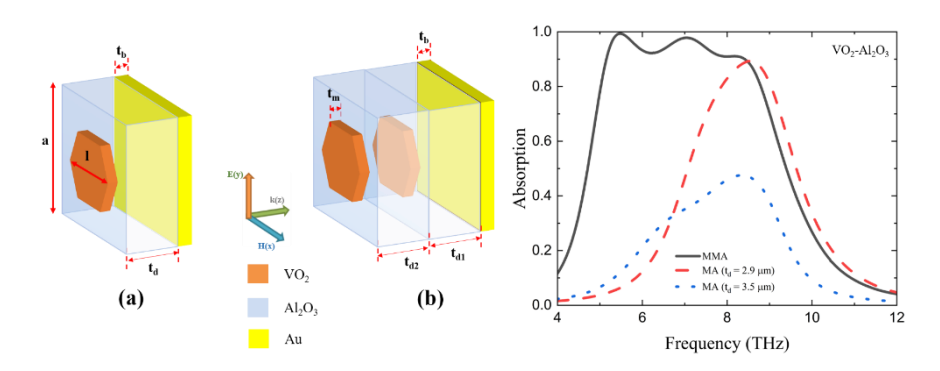


Figure 4.1. (a) Schematic of the single-layer MA structure, (b) Two-layer MMA structure with a VO<sub>2</sub> absorber layer, and (c) Absorption spectra of MMA and single-layer MA.

To examine the influence of Ohmic losses on absorption capability, a  $VO_2$ -Al<sub>2</sub>O<sub>3</sub> MMA structure was initially designed, showing three absorption peaks at 5.48 THz, 7.04 THz, and 8.31 THz (with absorbances of 99.34%, 97.83%, and 90.79%, respectively). The  $VO_2$  conductivity was then adjusted to 25.000 S/m to clarify this influence, resulting in a new set of three peaks at 6.68 THz, 9.24 THz, and 10.7 THz (with absorbances of 99.61%, 97.54%, and 98.35%, respectively).

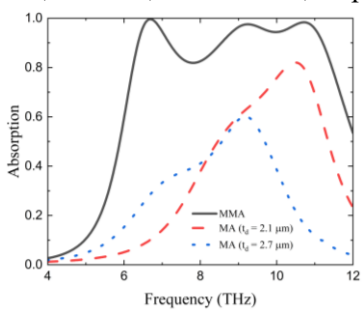


Figure 4.7. Absorption spectra of MA and MMA with a VO<sub>2</sub> (25000 S/m) absorber layer

# 4.2. Influence of the dielectric on the interaction

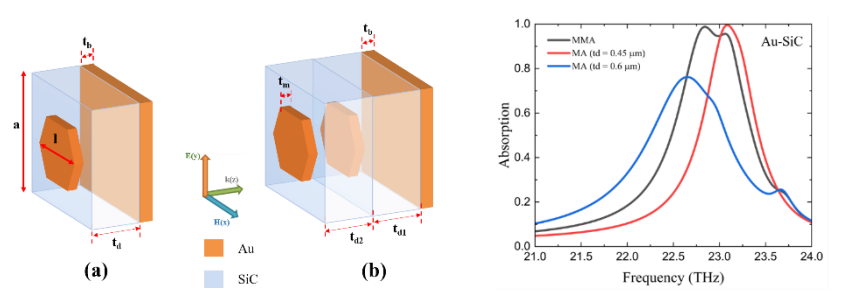


Figure 4.11. (a) Schematic of the Au-SiC MA structure, (b) Schematic of the MMA structure, and (c) Absorption spectra of the Al-SiC MA and MMA.

The Au-SiC MMA structure was proposed, as shown in Figure 4.11. The MMA exhibits two maximum absorption peaks at 22.84 THz and 23.06 THz, with corresponding absorbances of 98.77% and 95.62%. The absorption bandwidth exceeding 90% absorbance achieved an FBW value of 1.78%.

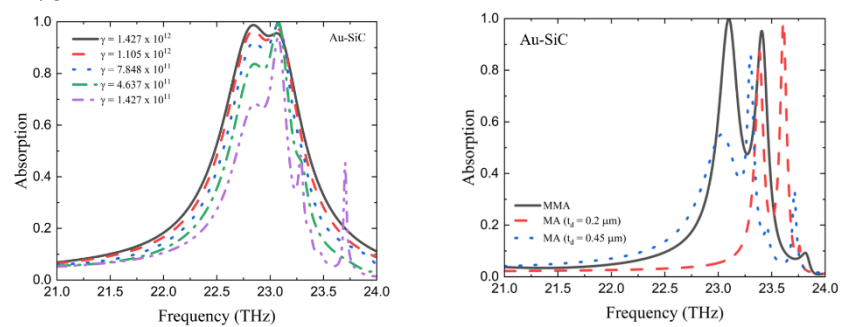
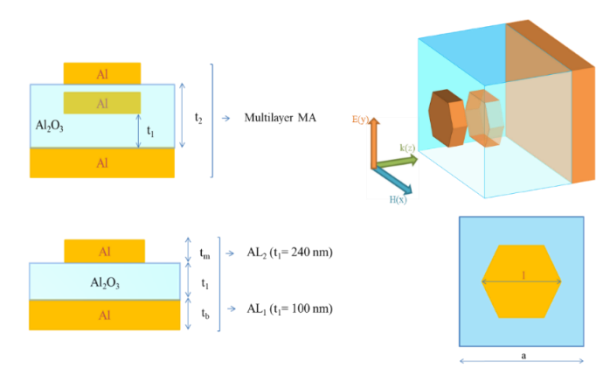


Figure 4.17. Influence of the dielectric loss coefficient  $\gamma$  on the absorption properties of the MMA, and the absorption spectra of the MMA and single-layer MA with  $\gamma$ =1.427×1011

The absorption spectra of the Au-SiC MA and MMA structures with  $\gamma$ =1.427  $\times$  10<sup>11</sup> are presented in Figure 4.17. The MMA structure exhibits two absorption peaks at frequencies of 23.09 THz and 23.4 THz, achieving absorbance values of 99.96% and 95.21%, respectively.

# 4.3. Application of MMA in Infrared Emission



**Figure 4.23.** Simulated unit cell structure of the single-layer hexagonal MA (bottom) and the multilayer MA (top) operating in the THz frequency range.

The unit cell of the proposed MMA has a size a and consists of two layers. The structural parameters of the unit cell were optimized with the following values: a=1500nm,  $t_b=200$ nm,  $t_l=100$ nm,  $t_m=100$ nm,  $t_2=240$ nm, and  $t_m=100$ nm.

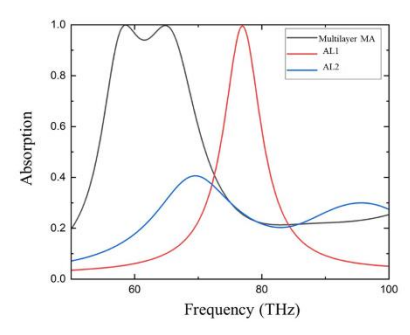


**Figure 4.24.** Absorption spectra of the single-layer hexagonal MA with varying thicknesses and the MMA structure.

Figure 4.24 presents the absorption spectra of the proposed MMA and the single-layer hexagonal MA. The results show that structures AL1 ( $t_I$  = 100 nm) and AL2 ( $t_I$  = 240 nm) exhibit two absorption peaks at 41.3 THz and 69.5 THz, with corresponding absorbances of 94% and 40%, respectively. The AL1 + AL2 structure yields superior

simulated absorption spectra, achieving an absorbance greater than 90% within the 56.9–67.9 THz frequency range.

# 4.3. Conclusion of Chapter 4

The chapter clarified inter-layer interaction by investigating MMAs with varying Ohmic losses and the influence of dielectric loss in the THz frequency range:

- High Ohmic Loss (VO<sub>2</sub>-Al<sub>2</sub>O<sub>3</sub>): The MMA achieved broadband absorption (FBW=47.89%), maintaining >90% absorbance between 5.16-8.41THz ( $\sigma$ =17500S/m).
- Low Ohmic Loss (VO<sub>2</sub>-Al<sub>2</sub>O<sub>3</sub>,  $\sigma$  = 25000S/m): The electromagnetic properties were simulated.
- Dielectric Loss (Au-SiC): Simulation of high- and low-loss MMAs showed that the high-loss case resulted in two absorption peaks.

# CHAPTER 5. RESEARCH ON MULTILAYER MULTIFUNCTIONAL METAMATERIAL STRUCTURES

# 5.1. Research on multilayer multifunctional metamaterial structures operating in the ghz frequency range

The multi-functional MMA structure is designed with three different single-layer MA structures, as shown in Figure 5.1. The structural parameters are presented in Table 5.1.

When the distance between the layers was optimized, the MMA achieved a maximum absorption spectrum value of 94.36% at a frequency of 4.36 GHz, and subsequently, the absorption decreased when  $d_1$ =3 mm.

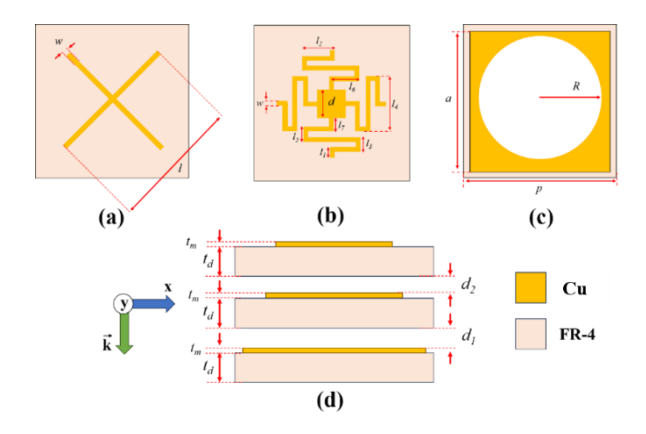


Figure 5.1. Schematic diagram of the design of a multi-functional MMA structure operating in the GHz frequency range, showing (a) the top layer, (b) the middle layer, (c) the bottom layer, and (d) the overall structure.

Parameters	p	$t_d$	$t_m$	а	R
Value (mm)	15	0.4	0.035	13.5	6
Parameters	d	$l_1$	$l_2$	$l_3$	$l_4$
Value (mm)	2.5	1.5	3	1.5	7
Parameters	$l_5$	$l_6$	$l_7$	w	l
Value (mm)	1.5	3	1	0.5	12

Table 5.1. Structural parameters of MMA operating in GHz region

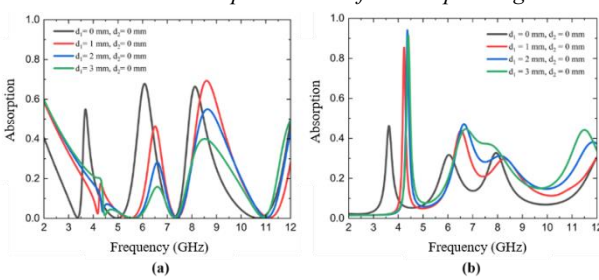


Figure 5.3. Transmission spectrum (a) and absorption spectrum (b) of the MMA structures

# 5.2. Research on multi-layer multi-functional metamaterial structure operating in the THz frequency range

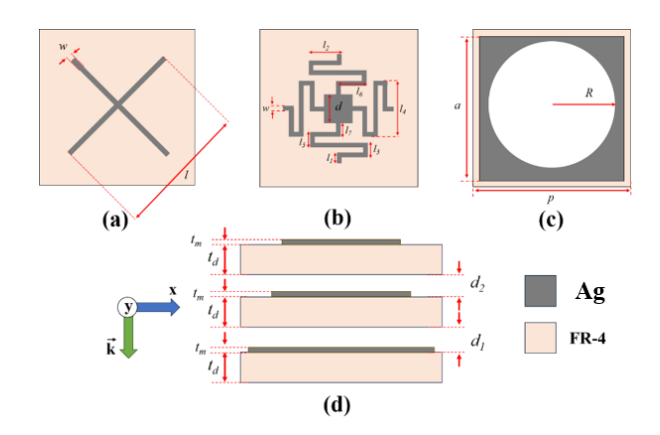


Figure 5.6. Schematic diagram of the design of a multi-functional MMA structure operating in the THz frequency range, showing (a) the top layer, (b) the middle layer, (c) the bottom layer, and (d) the overall structure.

The multi-functional MMA structure operating in the THz range is designed similarly to the MMA structure operating in the GHz range mentioned above. The structural parameters are presented in Table 5.2.

Parameters	p	$t_d$	$t_m$	а	R
Value (mm)	15	0.4	0.035	13.5	6
Parameters	d	$l_{I}$	$l_2$	$l_3$	$l_4$
Value (mm)	2.5	1.5	3	1.5	7
Parameters	<i>l</i> <sub>5</sub>	$l_6$	$l_7$	w	l
Value (mm)	1.5	3	1	0.5	12

Table 5.2. Structural parameters of MMA operating in THz region

When the distance between the layers of the MMA was optimized, the absorption spectrum reached a maximum value of 98.21% at a frequency of 5.29 THz.

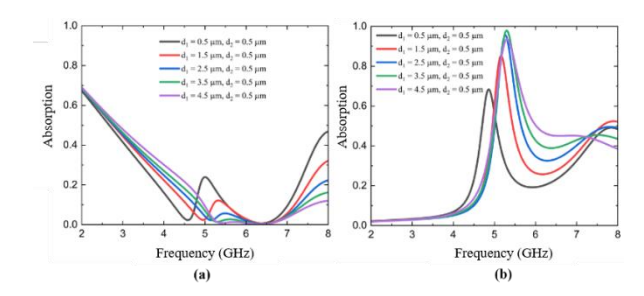


Figure 5.8. Transmission spectrum (a) and absorption spectrum (b) of the MMA structures with  $d_2$ =0.5  $\mu$ m and varying  $d_1$ 

## 5.3. Conclusion of Chapter 5

Based on the conversion effect between EIT and EIA, a multifunctional MMA operating in the GHz frequency range was designed and simulated. The multi-functional MMA was designed with three layers of single-layer MA structures. The absorption spectrum achieved a maximum value of 94.36% at a frequency of 4.36 GHz.

A multi-functional MMA operating in the THz frequency range was also designed and simulated. The absorption spectrum achieved a maximum value of 98.21% at a frequency of 5.29 THz. The surface current distribution was also simulated and investigated to clarify the interaction between the layers.

## **Overall Conclusion**

In this dissertation, multilayer metamaterial absorber (MMA) structures with different levels of Ohmic and dielectric losses were successfully designed, fabricated, and simulated.

- MMA structures operating in the GHz and THz frequency ranges were successfully developed. The Cu-FR4 based MMA exhibited two absorption peaks at 4.89 and 4.97 GHz with absorbances of 98.99% and

- 98.44%, respectively. The bilayer graphene-FR4 MMA achieved an absorption exceeding 90% over the 6.07-14.5 GHz range (FBW = 81.96%).
- A VO<sub>2</sub>-Al<sub>2</sub>O<sub>3</sub>-based MMA operating in the THz range was designed and simulated. When  $\sigma$  = 25000 S/m, the structure exhibited three absorption peaks at 6.68, 9.24, and 10.7 THz with nearly 100% absorbance. When  $\sigma$  = 17500 S/m, broadband absorption was maintained (FBW = 47.89%), with absorbance exceeding 90% in the 5.16–8.41 THz range.
- Multifunctional MMA structures comprising three single-layer MA designs using Cu-FR4 (GHz range) and Ag-PET (THz range) were also developed. These structures demonstrated the ability to switch between Electromagnetically Induced Transparency (EIT) and Electromagnetically Induced Absorption (EIA), achieving transmission levels of 55–69% and maximum absorbances of 94.36% (GHz) and 92.7% (THz).
  - The interlayer interaction mechanism was clarified, showing that:
- + Resonant layers with identical configurations lead to multiresonance phenomena, broadening the absorption bandwidth.
- + High Ohmic and dielectric losses cause absorption peaks to converge, resulting in broader bandwidths, while low losses lead to distinct separated peaks.
- + Adjusting the interlayer spacing allows control of the coupling behavior-from destructive to constructive interference-enabling tunable switching between EIT and EIA effects.

These findings provide significant insights into the development of high-performance multilayer MMAs with strong absorption efficiency and promising applications across both GHz and THz frequency ranges.

## **FUTURE RESEARCH DIRECTIONS**

- 1. Use machine learning techniques and AI to optimize MMA structures.
- 2. Apply new techniques and integrate advanced materials in MMA fabrication.
- 3. Research and apply MMA structures for energy harvesting and gas sensing.

#### LIST OF PUBLICATIONS RELATED TO THE THESIS

- 1. Bui Xuan Khuyen, Ngo Nhu Viet, Pham Thanh Son, Bui Huu Nguyen, Nguyen Hai Anh, Do Thuy Chi, Nguyen Phon Hai, Bui Son Tung, Vu Dinh Lam, Haiyu Zheng, Liangyao Chen and Youngpak Lee, "Multi-layered metamaterial absorber: electromagnetic and thermal characterization", Photonics, 11, No. 3, p. 219 (2024).
- 2. Bui Son Tung, Ngo Nhu Viet, Bui Xuan Khuyen, Thanh Son Pham, Phong Xuan Do, Nguyen Thi Hoa, Vu Dinh Lam and Do Khanh Tung, "Multiband and polarization-insensitive electromagnetically-induced transparency based on coupled-resonators in a metamaterial operating at GHz frequencies", Phys. Scr., 99 115502 (2024).
- 3. Thuy Chi Do, Bui Xuan Khuyen, Bui Son Tung, Ngo Nhu Viet, Duong Thi Ha, Vu Thi Hong Hanh, Xuan Phong Do, Do Khanh Tung\*, Hai Anh Nguyen and Vu Dinh Lam, "Wide-angle electromagnetic wave absorption via multilayer metamaterial structures", Phys. Scr., 100 025538 (2025)
- 4. Bui Son Tung, Ngo Nhu Viet, Bui Xuan Khuyen, Hai Anh Nguyen, Nguyen Khanh Viet, Phuc Vinh Nguyen, Vu Thi Van Anh and Vu Dinh Lam, "A bilayer metamaterial structure utilizing graphene ink for wide-band absorption in the GHz region", Phys. Scr., 100 085507 (2025)
- 5. Ngo Nhu Viet, Vu Dinh Lam, Bui Son Tung, Bui Xuan Khuyen, Pham Thanh Son, Nguyen Hai Anh, Nguyen Phon Hai, Do Khanh Tung, Do Thuy Chi, "Expanding the absorption bandwidth with two-layer graphene metamaterials in gigahertz frequency range", Comm. Phys., vol. 34, no. 4, p. 365 (2024).
- 6. Ngo Nhu Viet, Bui Xuan Khuyen, Vu Dinh Lam and Bui Son Tung, "Multilayer metamaterial absorber for infrared emitter application", Proceedings of IWNA, 08-11 (2023)